Estimation of ash injection in the atmosphere by basaltic volcanic plumes: the case of the Eyjafjallajökull 2010 eruption

Estimation of ash injection in the atmosphere by basaltic volcanic plumes: The case of the Eyjafjallajökull 2010 eruption

E. Kaminski,[1] S. Tait,[1] F. Ferrucci,[1,2] M. Martet,[3] B. Hirn,[4] and P. Husson[3]

Received 8 February 2011; revised 1 July 2011; accepted 26 July 2011; published 13 October 2011.

[1] During explosive eruptions, volcanic plumes inject ash into the atmosphere and may severely affect air traffic, as illustrated by the 2010 Eyjafjallajökull eruption. Quantitative estimates of ash injection can be deduced from the height reached by the volcanic plume on the basis of scaling laws inferred from models of powerful Plinian plumes. In less explosive basaltic eruptions, there is a partitioning of the magma influx between the atmospheric plume and an effusive lava flow on the ground. We link the height reached by the volcanic plume with the rate of ash injection in the atmosphere via a refined plume model that (1) includes a recently developed variable entrainment law and (2) accounts for mass partitioning between ground flow and plume. We compute the time evolution of the rate of injection of ash into the atmosphere for the Eyjafjallajökull eruption on the basis of satellite thermal images and plume heights and use the dispersion model of the Volcanic Ash Advisory Center of Toulouse to translate these numbers into hazard maps. The classical Plinian model would have overestimated ash injection by about 20% relative to the refined estimate, which does not jeopardize risk assessment. This small error was linked to effective fragmentation by intense interactions of magma with water derived from melting of ice and hence strong mass partitioning into the plume. For a less well fragmented basaltic dry eruption, the error may reach 1 order of magnitude and hence undermine the prediction of ash dispersion, which demonstrates the need to monitor both plume heights and ground flows during an explosive eruption.

Citation: Kaminski, E., S. Tait, F. Ferrucci, M. Martet, B. Hirn, and P. Husson (2011), Estimation of ash injection in the atmosphere by basaltic volcanic plumes: The case of the Eyjafjallajökull 2010 eruption, *J. Geophys. Res.*, *116*, B00C02, doi:10.1029/2011JB008297.

1. Introduction

[2] On the 14 April 2010, after about a month of effusive lateral eruption, the Eyjafjallajökull volcano, Iceland, switched to a more violent subglacial explosive eruption. The eruption produced a fluctuating volcanic plume (Figure 1) that was powerful enough to stun air traffic above Europe for a few weeks. Although remote sensing techniques allowing the detection of ash clouds have been continuously improved in recent years [e.g., *Tupper et al.*, 2004; *Clarisse et al.*, 2010; *Corradini et al.*, 2010], quantitative estimates of ash concentration in the cloud remain difficult and subject to some limitations. Hence, during a volcanic crisis such as the recent Icelandic one, one key issue remains the necessity that volcanologists provide robust estimates of the rate of ash injection into the atmosphere by the plume, a parameter required to estimate correctly the dispersion of ash by atmospheric currents, and the related necessity to close (or not) the airports.

[3] The continuous increase of computational resources and performances has allowed the development of 3-D models of turbulent volcanic plumes [e.g., *Textor et al.*, 2003; *Neri et al.*, 2007; *Suzuki and Koyaguchi*, 2009] that can be used to assess local volcanic hazard maps [e.g., *Cioni et al.*, 2003; *Esposti Ongaro et al.*, 2008]. The use of such complex models for the near real-time management of an eruption is, however, still out of reach. One-dimensional models of convective plumes provide simple scaling laws that relate the eruption rate, Q_0, to H, the height reached by the plume,

$$Q_0 = a H^4 + b, \tag{1}$$

where the values of the parameters a and b depend on the details of the modeling [e.g., *Wilson et al.*, 1978; *Glaze and Baloga*, 1996]. For example, the most recent series of models [*Kaminski et al.*, 2005; *Carazzo et al.*, 2008a] yields, for intermediate atmospheric conditions, $a = 74$ kg s^{-1} km^{-4} and $b = 0$ kg s^{-1} for $H \leq 12$ km, and $a = 258$ kg s^{-1} km^{-4} and $b = -4.6 \times 10^6$ kg s^{-1} for 12 km $\leq H \leq$ 17 km. Within the framework of Plinian eruptions, such that the magma is fully

[1]Institut de Physique du Globe, Sorbonne Paris Cité, CNRS UMR 7154, Université Paris Diderot, Paris, France.
[2]Department of Earth Science, Università della Calabria, Rende, Italy.
[3]VAAC Toulouse, Météo France, Toulouse, France.
[4]IES Consulting, Rome, Italy.

0148-0227/11/2011JB008297

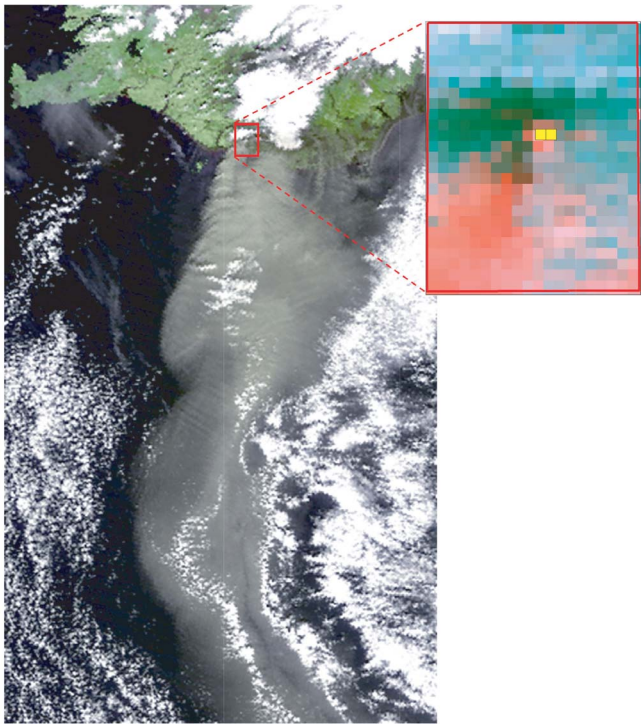

Figure 1. Satellite image of the Eyjafjallajökull ash plume, taken by Terra-MODIS in visible–near-infrared, at 12:50 UTC on 19 April 2010. The false color inset (MIR band 21, TIR band 31, TIR band 32) displays the near-source thermal structure of the plume and the two hot spot pixels (marked in yellow) used for the subresolution, dual-band estimate of the mass flow rate on the ground. The radiant flux from the hot spot pixels is $\approx 6 \times 10^8$ W, and the corresponding groundmass flow rate estimated from equation (20) is $\approx 2 \times 10^3$ kg s^{-1}.

fragmented in the volcanic conduit, the rate of injection of ash in the plume, Q_{ash}, is directly obtained from the eruption rate as a function of the mass fraction of gas in the magma, n_0,

$$Q_{\text{ash}} = (1 - n_0)Q_0 = (1 - n_0)\left(a H^4 + b\right), \tag{2}$$

where n_0 ranges between 2% and 7% for typical silicic magmas. These relationships applied at first order to explosive eruptions [*Sparks*, 1986], but natural data displayed some scatter not yet fully accounted for by models of Plinian plumes [*Mastin et al.*, 2009].

[4] The formation of convective plumes during Plinian eruptions is often associated with pyroclastic flows on the ground [*Kaminski and Jaupart*, 2001], whereas such as in the recent Icelandic example, basaltic explosive eruptions are often associated with effusive lava flows on the ground (Figure 2). In these two cases, the coexistence of an atmospheric plume with a ground flow implies a partitioning of the magma flux between the two flows. Hence, the proportionality between the rate of ash injection and the eruption rate (equation (2)) does not hold in general.

[5] The aim of this article is first to model the influence of mass partitioning between ground and atmospheric flows during an explosive eruption. We further show for the example of the Eyjafjallajökull eruption how the partitioning, and thus the effective ash flow rate, can be estimated from remote observations of the height of the plume and of the thermal output of effusive lava flow on the ground.

2. Integral Models of Turbulent Plinian Plumes

[6] The evolution of a turbulent plume formed above the vent during an explosive eruption can be described physically by (1-D) conservation equations, of mass, momentum and energy. Mass and momentum conservation are written using the top hat formalism and the concept of turbulent entrainment of *Morton et al.* [1956],

$$\frac{\mathrm{d}}{\mathrm{d}z}\left(\rho W L^2\right) = 2\rho_a U_e L, \tag{3}$$

$$\frac{\mathrm{d}}{\mathrm{d}z}\left(\rho W^2 L^2\right) = \left(\rho_a - \rho\right) g L^2, \tag{4}$$

where $W(z)$, $L(z)$, and $\rho(z)$ are the average vertical velocity, radius, and plume density, respectively, and $\rho_a(z)$ is the ambient air density. In the conservation of mass (3), $U_e = \alpha W$ is the rate of horizontal entrainment of ambient air into the plume, and the entrainment coefficient, $\alpha \approx 0.1$, characterizes

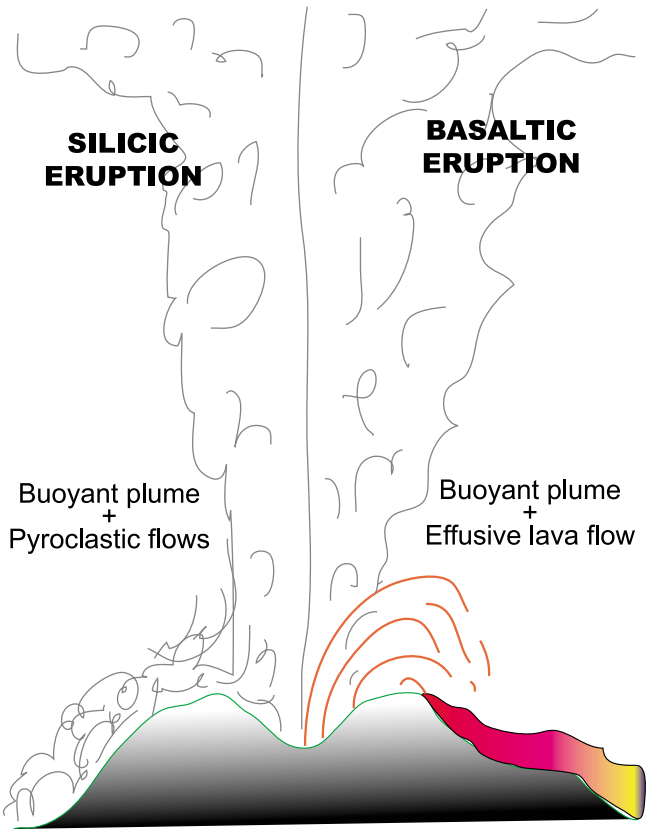

Figure 2. Schematic representation of explosive eruptions in which part of the magma is injected into a turbulent atmospheric plume and part is emitted on the ground as pyroclastic flows (silicic eruptions) and/or effusive lava flows (basaltic eruption). All the gas is exsolved and released into the plume.

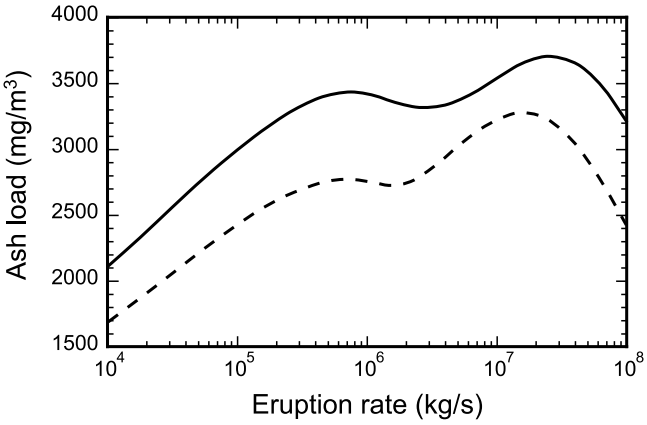

Figure 3. Influence of variable entrainment on the ash load at the top of the plume. A constant entrainment $\alpha_e = 0.1$ (dashed line) yields a smaller ash load than variable entrainment (solid line). This reflects the reduction of entrainment in this latter case due to the initial negative buoyancy of the volcanic jet.

the efficiency of turbulent entrainment of ambient air into the plume. We further use the conservation of energy proposed by *Woods* [1988],

$$\frac{\mathrm{d}}{\mathrm{d}z}\left(\rho C_p W L^2 T\right) = 2\rho_a U_e L\left(C_a T_a + \frac{1}{2}W^2\right) - \rho_a g W L^2, \qquad (5)$$

where $T(z)$ is the plume temperature, $T_a(z)$ and $\rho_a(z)$ are the ambient air temperature and density, respectively, C_a = 998 J K^{-1} kg^{-1} is air heat capacity, and g is the acceleration of gravity. The plume heat capacity is given by [*Woods*, 1988]

$$C_p = C_{p0} + \left(C_{p0} - C_a\right)\frac{1-n}{1-n_0}, \qquad (6)$$

where C_{p0} = 1617 J K^{-1} kg^{-1}. *Glaze et al.* [1997] proposed a more complete treatment of the conservation of energy that corrects some inconsistencies in the formulation of *Woods* [1988]. However, their refined model does not significantly affect the prediction of the total height of the plume; hence, we choose to use here the set of equations of *Woods* [1988] that remains the most widely used. This simplified model does not account for additional important parameters, such as the effect of wind [*Bursik*, 2001] or the influence of sedimentation and recycling of pyroclasts at the edges of the plume [e.g., *Veitch and Woods*, 2002]. It allows, however, studying the influence of the partitioning factor f, all other things being equal, and hence allows us to demonstrate that f is a key parameter to take into account in any modeling of volcanic plumes.

[7] The conservation equations are completed by an equation of state for the evolution of the density of the volcanic plume as a function of temperature and of the gas mass fraction n (or the ash mass fraction $x = 1 - n$) [*Woods*, 1988]

$$\frac{1}{\rho} = \frac{(1-n)}{\rho_m} + \frac{nR_g T}{P}, \qquad (7)$$

$$n = 1 + (n_0 - 1)\frac{\rho_0 W_0 L_0^2}{\rho W L^2}, \qquad (8)$$

$$R_g = R_a + \left(R_{g0} - R_a\right)\left(\frac{1-n}{n}\right)\left(\frac{n_0}{1-n_0}\right). \qquad (9)$$

where R_{g0} = 462 J K^{-1} mol^{-1} and R_a = 285 J K^{-1} mol^{-1} are the bulk plume and air gas constant, $\rho_m = 2.8 \times 10^3$ kg m^{-3} is the density of the bubble-free magma, P is the atmospheric pressure, and the subscript 0 refers to initial values of the variables at the vent.

[8] The solution of the above set of equations shows that the height reached by the plume, the ash load at the top of the plume, and the rate of ash injection into the atmosphere by the plume, all depend mainly on the mass flow rate, $Q_0 = \rho_0 W_0 L_0^2$ [see *Woods*, 1995, Figures 17 and 21], and secondly on the magma temperature and on the stratification of the atmosphere. In a recent set of models of turbulent entrainment in jets and plumes, our group [*Kaminski et al.*, 2005; *Carazzo et al.*, 2006] has demonstrated that the dynamics of the plume also depend on the entrainment coefficient α_e, that has further to be taken as a function of the plume buoyancy relative to the ambient atmosphere,

$$\alpha = \frac{0.135}{2} + 0.333\frac{gL^2}{W}\frac{(\rho_a - \rho)}{\rho}. \qquad (10)$$

We have shown that within this framework variable entrainment has a significant influence on the condition of collapse of Plinian columns [*Carazzo et al.*, 2008a] and on the height reached by the plume for a given eruption rate [*Carazzo et al.*, 2008b], but its role in determining the plume ash load has not been investigated yet.

[9] To quantify the influence of variable entrainment we consider a reference case, defined by a magma temperature of 1000°C, with 5 wt % of dissolved water, a sonic exit velocity of 300 m s^{-1}, and for increasing values of the mass flow rate from 10^4 to 10^8 kg s^{-1}. The atmospheric properties used are the same as those of *Woods* [1988] for midlatitude conditions. We do not study the influence of atmospheric properties because *Woods* [1995] showed that their impact is negligible if the plume's height remains below the tropopause, which is the case for the Eyjafjallajökull. We show in Figure 3 the difference between a case with a constant entrainment coefficient $\alpha_e = 0.1$ and a case with variable entrainment given by equation (10) for the rate of ash injection into the plume and the ash load at the top of the plume. We obtain that the ash load is larger in the case with variable entrainment. This is due to a smaller efficiency of entrainment due to the initial negative buoyancy of the volcanic jet (from equation (10)): at a given height, the plume has a slightly smaller cross section if entrainment is reduced and hence has a larger concentration of ash. One may note that the change in the ash load occurs at a constant rate of ash injection into the plume ($Q_{\mathrm{ash}} = (1 - n_0)Q_0$). The effect is not very large and is of same order as the effect of the eruption temperature [e.g., *Woods*, 1995].

[10] We conclude that in Plinian eruptions, characterized by efficient fragmentation, such that all of the magma and

magmatic gases are injected into the vertical jet above the vent, the observation of the height of the plume yields an estimate of the eruption rate through the scaling law 1. The eruptive flow rate provides in turn an estimate of the rate of ash injection once corrected for the gas content of the magma and an estimate of the ash load through Figure 3.

[11] We now consider more complex cases for which fragmentation is not efficient enough to entirely fragment the magmatic foam into ash injected into the plume at the vent. The eruptive plume is then associated with a ground flow that must be accounted for in the modeling.

3. Influence of the Partitioning Factor

3.1. Relationship Between the Height of the Plume and the Plume Flow Rate

[12] In the more general case where an eruption produces both a plume and a flow on the ground, the injection of fragmented magma into the plume is not total, but there is a partitioning of the mass flux between ground and atmospheric flows. To illustrate how this effect influences the dynamics of the plume and the subsequent estimate of ash injection into the atmosphere, we introduce an additional parameter into the previous model, a partitioning factor f, defined as the percentage of magma finely fragmented and injected into the plume.

[13] We consider that despite reduced fragmentation, the magmatic gas is fully exsolved at the vent and thus fully participates in the plume. Hence, the initial effective mass fraction of ash in the plume at the vent is x_f,

$$x_f = \frac{(f/100)(1-n_0)}{n_0 + (f/100)(1-n_0)}, \tag{11}$$

whereas the effective mass fraction of gas in the plume at the vent is n_f,

$$n_f = \frac{n_0}{n_0 + (f/100)(1-n_0)}. \tag{12}$$

The effective plume density ρ_f is given by

$$\frac{1}{\rho_f} = \frac{x_f}{\rho_m} + \frac{n_f R_g T}{P}. \tag{13}$$

Any flux X_0 (of mass, momentum, or energy) becomes X_f,

$$X_f = [n_0 + (f/100)(1-n_0)]X_0. \tag{14}$$

One should note that the reduced fluxes set the values of the velocity W_f and plume radius L_f after partitioning,

$$W_f = \frac{M_f}{Q_f}, \tag{15}$$

$$L_f = \left(\frac{Q_f}{\rho_f W_f}\right)^{0.5}. \tag{16}$$

where Q_f and M_f are the reduced mass and momentum fluxes, respectively, calculated from equation (14). The temperature in the plume is not affected by partitioning as the pyroclasts are at the same temperature as the gas.

[14] The partition factor f is linked to the fraction of fine material produced during an eruption, and can be related to the efficiency of fragmentation in the conduit. The fraction of fine material can be estimated from the grain size distribution of the population of pyroclasts produced during fragmentation. *Kaminski and Jaupart* [1998] have shown that the grain size distributions of Plinian eruptions follow a power law, such that the number N of fragments larger than a given size r_0 is $N(r \le r_0) \propto r_0^{-D}$. The exponent D of the distribution ranges between 3.9 for Plinian fall deposits and 2.8 for pyroclastic flow deposits, whereas the fragmentation of a pumice in the laboratory yields an exponent of 2.5. The size distribution if very sensitive to the value of D: if the exponent D of the distribution is larger than 3 fine material is much more abundant than coarse material, whereas it is the opposite for $D < 3$ [*Kaminski and Jaupart*, 1998]. If one defines fine material as having a size between 1 μm and 10 μm, and considers a total range of sizes between 100 cm and 1 μm, $D = 3.9$ yields $f \approx 88\%$, $D = 2.8$ yields $f \approx 4\%$ and $D = 2.5$ yields $f \approx 0.25\%$.

[15] The population of pyroclasts produced by basaltic eruptions is usually coarser than the population produced by silicic ones [e.g., *Rose and Durant*, 2009]; hence, basaltic eruptions are likely to be characterized by significantly smaller values of f. In Strombolian eruptions, for example, the quantity of gas (in wt %) in ash-poor plumes has been estimated to be larger than 67% and up to 95% [*Chouet et al.*, 1974; *Rose et al.*, 1980]. Such a small value is consistent with the observation by *Lane and Gilbert* [1992] of virtually ash-free plumes produced by the explosive activity of Sakurajima volcano in 1991. Models of basaltic plumes above basaltic eruptions have used f between 1% and 17% [e.g., *Woods*, 1993]. In the following we will consider a large range of variations, f = 1%–100%, to include both silicic and basaltic cases.

[16] All the bubbles disrupted at fragmentation release the gas they contain. However, if large fragments are produced at fragmentation, the bubbles they contain may trap a significant quantity of gas. *Thomas et al.* [1994] and *Kaminski and Jaupart* [1997] have demonstrated that the vesicularity of pumice shows systematic variations among andesitic Plinian eruptions, which were consistent with pumice expansion after fragmentation and hence with the presence of nonconnected bubbles inside the fragments. Permeability estimates for natural samples [*Klug and Cashman*, 1996] and in laboratory experiments [*Burgisser and Gardner*, 2005] indicate that permeability is minimum in violent Plinian eruptions of very viscous magma. On the other hand, permeability develops quite efficiently in less viscous and less violent eruptions, which will allow a rather complete degassing of the pumice. The hypothesis that all the magmatic gas participates in the plume is thus more likely to apply for basaltic sub-Plinian eruptions.

[17] To describe the influence of the partitioning factor on the dynamics of the plume, we first calculate the height of volcanic plumes with the same characteristics as before ($n_0 = 5$ wt %, $T_0 = 1000$°C, $W_0 = 300$ m s^{-1}, 10^4 kg s$^{-1} \le Q_0 \le 10^8$ kg s^{-1}), but for a partitioning factor f between 5% and 100%. We show in Figure 4 the maximal height H_f reached by the volcanic plume, as a function of the effective plume

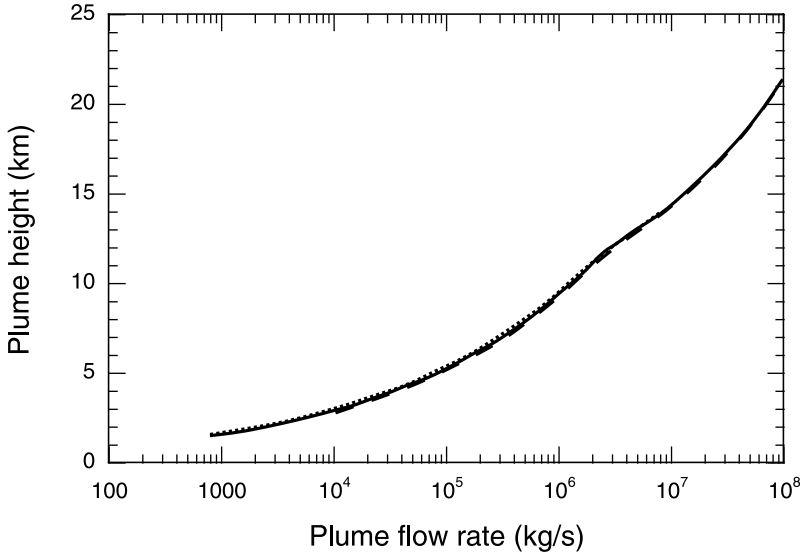

Figure 4. Evolution of the height of the volcanic plume as a function of its effective mass flow rate (gas plus ash) for $f = 100\%$ (dashed line) and $f = 5\%$ (dotted line). The solid line, defined by $H_f = 0.30\ Q_f^{0.25}$ for $H \leq 12$ km and $H_f = 5.53 + 0.16\ Q_f^{0.25}$ for $H \geq 12$ km, is fully consistent with classical scaling laws [*Carazzo et al.*, 2008a]. The influence of f is negligible because, independently of f, the volumetric fraction of ash is always small enough for the plume to be described as a dilute gas flow.

mass flow rate (gas plus ash), $Q_f = [n_0 + (f/100)(1 - n_0)]Q_0$. The results are well described by a classical scaling law

$$H_f = 0.30\ Q_f^{\frac{1}{4}}, \quad H \leq 12 \text{ km}, \tag{17}$$

$$H_f = 5.53 + 0.16\ Q_f^{\frac{1}{4}}, \quad H \geq 12 \text{ km}. \tag{18}$$

The negligible effect of f on the height of the plume for a given flow rate is to be related to the fact that the volumetric fraction of ash is always small enough for the plume to be considered as a dilute gas flow [*Woods*, 1995] whose properties depend only on the ratio between magmatic gas and ambient air (through equation (9)).

[18] Figure 4 shows that the height of the volcanic plume always provides a robust estimate of the plume mass flow rate. However, the important parameter for the modeling of ash dispersion is not the total plume mass flux but rather the fraction of ash in the plume. Hence, we now consider the relationship between the height of the plume and its ash content.

3.2. Relationship Between the Height of the Plume and Its Ash Content

[19] For a given plume flow rate at the vent, $Q_f = [n_0 + (f/100)(1 - n_0)]Q_0$, and neglecting sedimentation from the plume's margins, the rate of ash injection into the atmosphere by the plume is $Q_{\text{ash}} = (f/100)(1 - n_0)Q_0$. We show in Figure 5 the relationship between the height of the plume and the mass flux of ash in the plume. It appears that the height of the plume does not fully constrain the ash injection rate into the plume. This must be the case because as shown in Figure 4, the height of the plume in controlled by its total mass flow rate (gas plus ash), independently of f. For example, a height of 9.5 km may correspond to a rate of ash injection into the plume between 10^6 kg s^{-1} for a fully efficient fragmentation ($f = 100\%$) to 1.7×10^5 kg s^{-1} for the minimum value of f (1%). Hence, the parameters of equation (2) corresponding to Plinian eruptions ($f \approx 100\%$) should not be used to estimate the ash flow rate in plumes produced by basaltic eruptions in which $f \leq 10\%$ may be typical.

[20] Similarly, we plot in Figure 6 the ash load at the top of the plume, defined as the product of the mass fraction of ash $(1 - n)$ by the density of the plume (ρ), as a function of the plume height and for a partitioning factor increasing from 1% to 100%. Figure 6 shows that the knowledge of the height of the plume provides a poor estimate of the ash load at the top of the plume, because the partitioning factor f has an important effect. The use of a classical Plinian model without knowing the value of f, may yield an overestimate of almost on order of magnitude of the ash content. For example, a plume 12 km high may correspond to an ash load varying from about 450 mg m^{-3} for $f = 1\%$ to ≈1500 mg m^{-3} for $f = 5\%$ and up to ≈3200 mg m^{-3} for $f = 100\%$. Changes in the ash concentration appear very sensitive to f when it is below 10%, i.e., in the case of basaltic eruptions.

[21] After the Eyjafjallajökull crisis, the International Civil Aviation Organization (ICAO) determined that flight is allowable in areas of low ash concentration (≤2 mg m^{-3}) and prohibited in areas of high ash concentration (≥4 mg m^{-3}). All things being equal, a change of f from 100% to 10%, or a change of f from 2% to 1%, would yield a decrease by a factor of two in the ash content of the eruptive cloud. These results demonstrate that when the volcanic plume is associated with a significant flow on the ground ($f \leq 10\%$), one must not neglect the influence of the partitioning of the erupted mass between the atmosphere and ground flow.

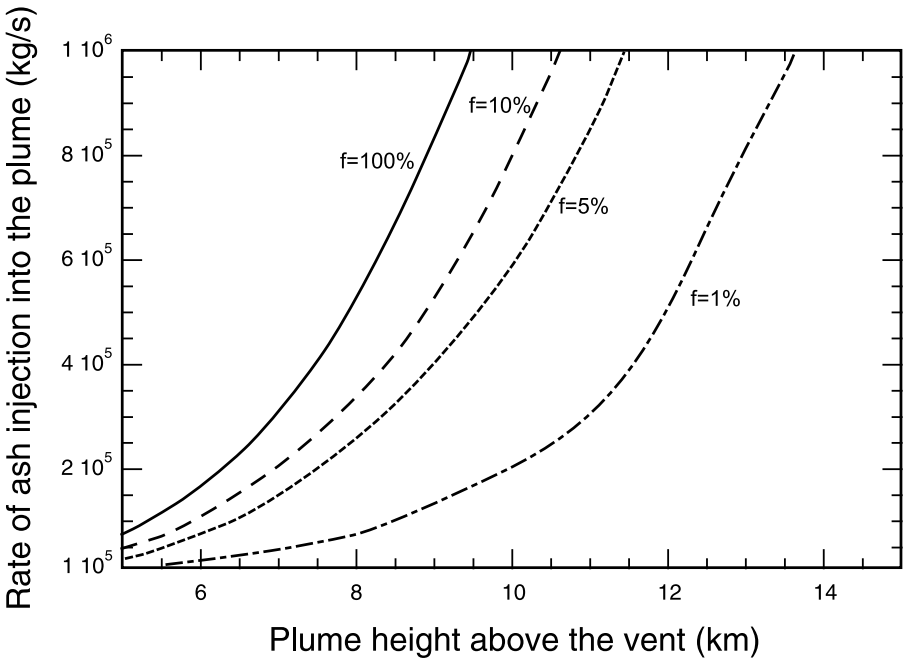

Figure 5. Relationship between the height of the plume and the rate of ash injection into the plume for various values of the partitioning parameter *f*. If *f* is not known, the observed height of the plume combined with the Plinian model (*f* = 100%) is not sufficient to obtain a robust estimate of the rate of ash injection. Applied to a basaltic eruption with a small *f*, the Plinian model will imply an overestimation that can reach 1 order of magnitude.

3.3. Estimates of Ground Flow Mass Fluxes and of the Partitioning Factor

[22] Techniques have recently been developed to estimate the ash content of plumes using radar Doppler technics [*Gouhier and Donnadieu*, 2008], but these have been applied so far to Strombolian volcanoes only, i.e., involving sporadic explosions rather than a sustained turbulent jet. Hence, in general, the ash content of an explosive plume

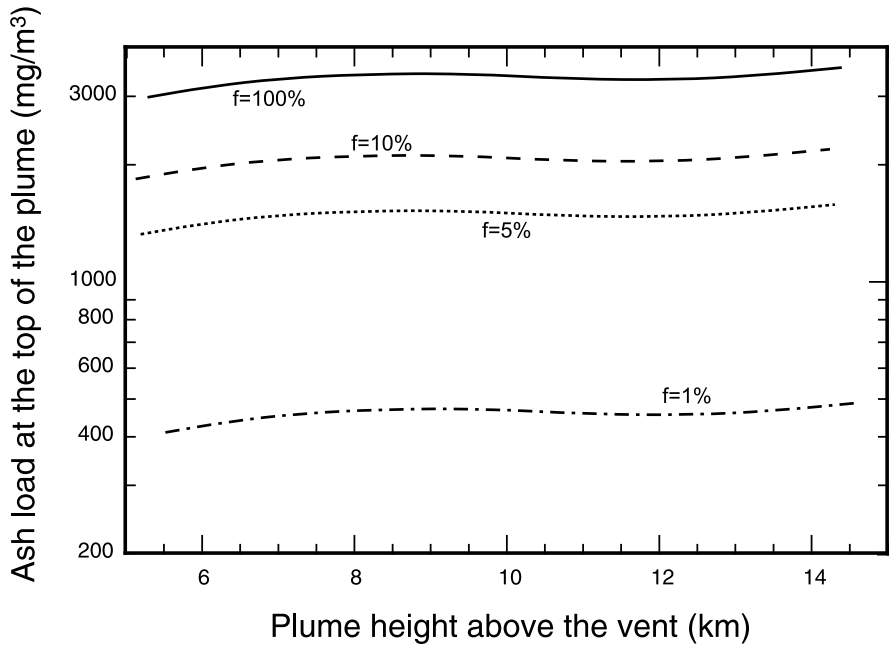

Figure 6. Relationship between the height of the plume and the ash load of the top of the plume for various values of the partitioning parameter *f*. The ash load shows only a weak variation with the height of the column and is mainly controlled by *f*.

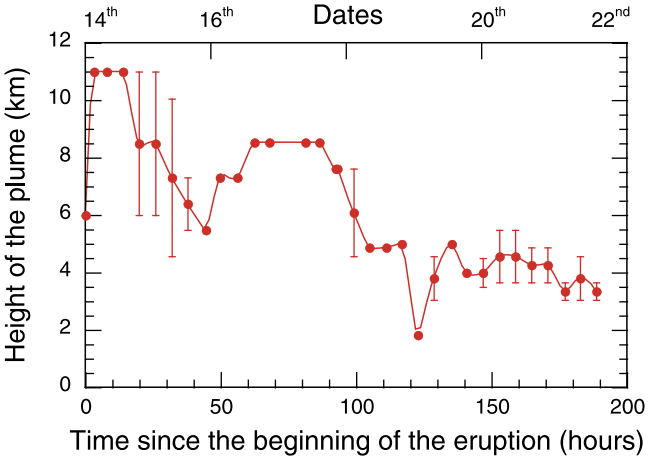

Figure 7. Evolution of the height of the Eyjafjallajökull plume as a function of time between 14 and 22 April 2010. The data are from the Icelandic Meteorological Office and the London Volcanic Ash Advisory Center. The error bars correspond to the variability of the plume height, for example, due to a strong wind [*Petersen*, 2010], and to the uncertainty linked to the method employed (see *Tupper and Wunderman* [2009] for a general discussion of the assessment of the height of volcanic plumes).

will require the knowledge of both the plume mass flow rate and the ground flow rate.

[23] When volcanoes are monitored by observatories, direct visual measurements in the field can provide rough estimates of the effusive mass flow rates. For example, a value of 3×10^4 kg s^{-1} was estimated for the average effusive flow rate of Eyjafjallajökull during the April 2010 episode by the teams of the Icelandic Meteorological Office and Institute of Earth Sciences of the University of Iceland. When such direct methods cannot be relied on, other observations must be used as a proxy for the eruptive flow rates.

[24] In the case of pyroclastic flows, the key observable is the distance covered by the flow on the ground, d (m), that can be related to the mass flux of the ground flow Q_g (kg s^{-1}), as [e.g., *Bursik and Woods*, 1996]

$$Q_g = cd^2, \tag{19}$$

where $c \approx 4.5$ kg s^{-1} m^{-2} for a dilute flow, and about 10 kg s^{-1} m^{-2} for a concentrated one [*Carazzo et al.*, 2008b].

[25] For effusive lava flows, semiempirical laws relate the mass flow rate Q_g to the radiated thermal energy, F_g (W) [*Wright et al.*, 2001; *Harris et al.*, 2007; *Hirn et al.*, 2009]

$$Q_g = \frac{F_g}{C_p \Delta T + \Phi C_L}, \tag{20}$$

where the parameters are $\Delta T \approx 200$°C is the average temperature drop throughout the active flow, $\Phi = 0.4$–0.5 is the average mass fraction of crystals, $C_p \approx 1.2\ 10^4$ J kg^{-1} K^{-1} is specific heat capacity, and $C_L \approx 3\ 10^5$ J kg^{-1} K^{-1} is latent heat of crystallization [*Wright et al.*, 2001].

[26] If both the ground flow rate Q_g and the plume flow rate Q_f have been obtained from the runout distance or the thermal radiance and from the plume's height, respectively, then

$$f = \frac{100}{1 - n_0}\left(\frac{Q_f}{Q_0} - n_0\right), \tag{21}$$

where $Q_0 = Q_g + Q_f$ is the total flow rate. For fractions of dissolved gas below 10%, and given the often large error bars of flow rate estimates, the partitioning factor can be reasonably approximated as

$$f \approx 100\,\frac{Q_f}{Q_f + Q_g}. \tag{22}$$

Once the partitioning factor f has been estimated, it can be combined with the plume height to obtain the ash flow rate and the ash load of the plume from Figures 5 and 6, respectively, as illustrated below for the recent Eyjafjallajökull eruption.

4. Modeling the Rate of Injection of Ash Into the Atmosphere During the Eyjafjallajökull Eruption

[27] The first information required to estimate the rate of injection of ash during an explosive eruption is the height of the plume. During the more violent explosive episode of the Eyjafjallajökull eruption, that lasted from the 14 to 22 April (the eruption ended on 22 May), the height of the plume was reported daily by the Icelandic Meteorological Office (IMO) and London Volcanic Ash Advisory Center (VAAC) (Figure 7 and Table 1). We changed these values into a plume mass flux by taking into account the altitude of the volcano (1.66 km) and using equation (17) (Figure 8). The calculation shows that the plume flow rate decreases from 10^6 kg s^{-1} on 14 April to 3×10^4 kg s^{-1} on 18 April to 10^3 kg s^{-1} on 22 April.

[28] The average effusive flow on the ground during the first three days of the explosive episode was estimated to be around 3×10^4 kg s^{-1} by the staff of the Institute of Earth Sciences (IES) of the University of Iceland (http://www.earthice.hi.is/). Because of major cloud cover during that period, and the inherent lack of visibility at all wavelengths, remote sensing unfortunately cannot be used to refine the average estimate. In the following days, the IES estimates that the eruptive flow rate decreased by 1 order of magnitude. Satellite images confirm this decrease and allow us to estimate the effusive flow rate. Between 19 and 22 April, the flow rate varies by less than a factor of 2, and within error bars can be taken as constant, and equal to 2×10^3 kg s^{-1} (Figure 1).

Table 1. Average Eruptive Parameters for the 18–22 April Explosive Episode of the Eyjafjallajökull 2010 Eruption[a]

Plume Height (km)	Plume Flow Rate (kg s^{-1})	Effusive Flow Rate (kg s^{-1})	Partitioning Factor (%)	Ash Flow Rate (kg s^{-1})
11	10^6	3×10^4	97	9.5×10^5
8.5	3×10^5	3×10^4	91	2.8×10^5
6	3×10^4	3×10^3	91	2.8×10^4
3	10^3	2×10^3	33	8.6×10^2

[a]Effusive flow rates are from the Icelandic Meteorological Office and the Institute of Earth Sciences, University of Iceland.

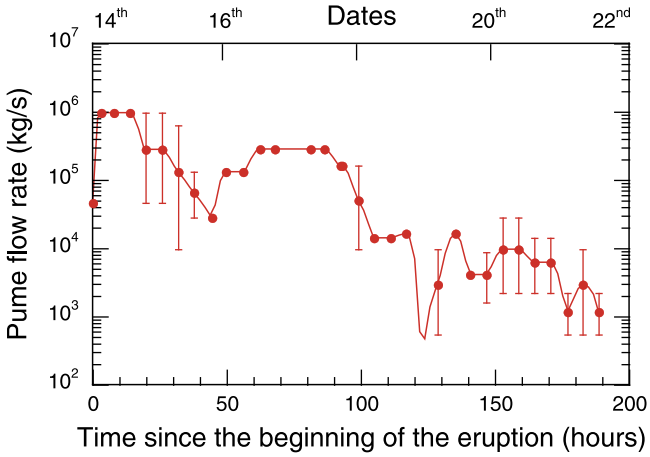

Figure 8. Time evolution of the Eyjafjallajökull plume flow rate over the same period as in Figure 7.

[29] The values of the plume flow rate and of the ground flow rate inferred above yield a partitioning factor f of 97% at the beginning of the eruption, 91% on 19 April, and 33% by 22 April. Hence, the rate of ash injection (from Figure 5) decreased from 9.5×10^5 kg s^{-1} at the beginning of the eruption to less than 9×10^2 kg s^{-1} on 22 April (Table 1), i.e., a variation of about 3 orders of magnitude. Such a small value is first due to the decrease of the plume flow rate and then also to the decrease of the partitioning factor. To illustrate the effect of large variations of the rate of ash injection on hazard assessments for air traffic, we further calculated ash dispersion in the atmosphere.

[30] We used the "MOCAGE-accident" dispersion model of Météo France, which is a specific version of MOCAGE (Modèle de Chimie Atmosphérique à Grande Échelle), a three-dimensional chemistry and transport model developed by Météo France to predict transport and diffusion of accidental release, from the regional to the global scale. In the version of the model used, only dynamical and physical processes are taken into account, and not chemistry. Sedimentation of ash is taken into account using tracers. Meteorological forcing (hydrostatic winds, temperature, humidity and pressure) is obtained from Météo France operational products every 6 h and linearly interpolated on an hourly basis, to compute advection with a semi-Lagrangian scheme. MOCAGE-accident can be run for an emission taking place everywhere over the globe. In the operational configuration, it has a horizontal resolution of 0.5 degrees, and 47 hybrid levels from the surface up to 5 hPa, with approximately 7 levels in the planetary boundary layer, 20 in the free troposphere and 20 in the stratosphere. Additional information on MOCAGE-accident is given by *Witham et al.* [2007], who present the results of an intercomparison of VAAC dispersion models conducted in 2005 after the Grimsvötn Icelandic eruption.

[31] We considered two cases with two different rates of injection: a rate of 2×10^5 kg s^{-1} for case 1, and a rate of 2×10^4 kg s^{-1} for case 2. All the other parameters (plume height of 8 km, average grain size of 10 μm) are kept constant. For the sake of argument, we consider a constant rate of injection over 24 h, and we model the ash dispersion after three days, using the atmospheric conditions above Iceland between 5 and 8 May. The resulting maps, drawn in Figure 9, show that the two cases yield a similar pattern for the dispersion of the ash cloud but, as expected, a difference of a factor of 10 in the concentration of ash in the zone of highest density of ash. The variation of the source has thus a direct impact on the modeling of ash dispersion, and is not erased by mixing and dispersion by atmospheric currents. Such an error in the source term used in VAAC forecasting may thus account for the differences between model prediction and observations during the Eyjafjallajökull eruption, as suggested recently by *Mastin et al.* [2010].

[32] From the calculations presented in Figure 9, one can propose a simple relationship between the rate of ash injection by the plume, A_f, in kg s^{-1}, and the mass of ash per unit area, M_a in t km^{-2}. By integrating the average ash concen-

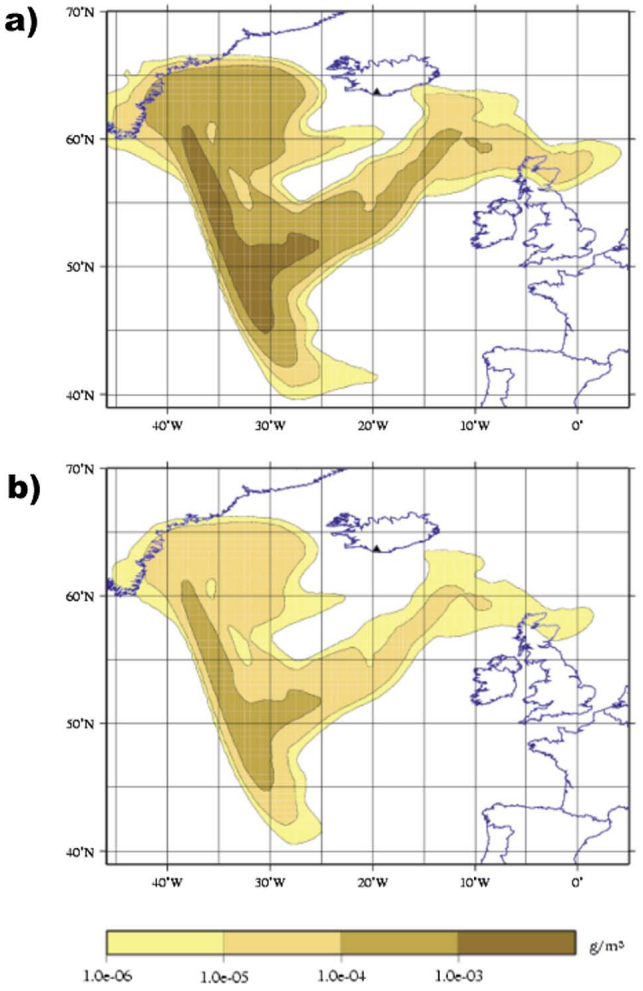

Figure 9. Predictions of ash dispersion above Iceland, given as average ash concentration in the column between 1.5 and 8 km, for 1 day of injection and 3 days of dispersion corresponding to atmospheric conditions between 5 and 8 May. Two rates of ash injection into the atmosphere are considered: (a) 2×10^5 kg s^{-1} and (b) 2×10^4 kg s^{-1}. The zones affected by the ash cloud are similar in the two cases, but the ash concentration is 10 times larger in the central part of the cloud for Figure 9a.

tration over the whole column (between 1.5 and 8 km in our example), we obtain

$$A_f \approx 3 \times 10^4 M_a. \quad (23)$$

On 17 April, the maximum ash concentration in the ash cloud was about 12 t km^{-2} [*Piscini et al.*, 2010], which yields an ash injection rate of about 3.5×10^5 kg s^{-1}. This value is about a third of the maximal rate of ash injection reached on 14 April (Table 1), but is quite close to the average rate for the 14–17 April period. After 20 April, the ash cloud was not detectable by satellites, which is interpreted as being due to the presence of meteorological clouds above the ash cloud [*Piscini et al.*, 2010]. This could also reflect an ash concentration below the detection threshold of the satellites, as the model predicts an ash concentration smaller than 0.6 t km^{-2}.

5. Conclusion

[33] The Eyjafjallajökull eruption was a subglacial explosive eruption, characterized by intense interactions with water derived from the melting of ice, that were likely to increase the efficiency of the fragmentation of the magma. As a result, the partitioning factor was close to 100% at the beginning of the eruption, and the Plinian model of the eruptive plume provided reasonable estimates for the ash content. In the less violent phases of the second week of the explosive episode, the decrease of the eruptive flow rate and of the partitioning factor yielded a decrease of about 3 orders of magnitude of the ash concentration predicted in the ash cloud. Hence, the assumption of a constant rate of injection of ash based on the first days of the eruption resulted in an overestimate of the risk induced for air traffic above Europe.

[34] In the absence of ice and/or for a less silicic magma, the partition factor would have been closer to the usual value for Strombolian eruptions, i.e., smaller than 10%. Small values of f are also expected for collapsing Plinian columns. In these cases, the "pure Plinian" model would yield overestimated rates of ash injection into the atmosphere. Hence, in general, a robust estimate of the release of ash into the atmosphere should be based not only on an observation of the plume height, but also at least on a first-order determination of the fraction of erupted material flowing on the ground.

[35] Satellite retrievals of ash concentration have been shown to be possible from instruments such as SEVIRI, which have very high refreshment rates, notably during the Eyjafjallajökull eruption of 2010 [e.g., *Thomas and Prata*, 2011]. Nevertheless, the ash concentration is too high in the near source region for this approach to work, and one must wait until the cloud is someway downwind and hence diluted before ash concentration can be measured in this way. So although this quasi-real-time information is undoubtedly useful its main application is to allow rerouting of aircraft already in the air. For the management of a crisis of longer duration, the ideal information to have is some quantitative estimate of the distribution of ash concentration in the atmosphere ahead of time. This requires running a dispersion model such as MOCAGE, as indeed is currently done by the VAACs in order to forecast ash distribution. However, accurate information on the ash concentration in the volcanic source region is required for this approach to be really a powerful crisis management tool. Local observers can provide some rough visual estimates on what is happening at the source, but there are important limitations. First, "local" observations are only really possible when the event is not so violent that local observation becomes impossible. In the effusive case, one might estimate how much lava is emitted in a given time interval. In the case of explosive activity, the amount of ash sedimented in a given time interval can be observed, but this does not indicate how much ash might be injected into the atmosphere without supplementary information on the grain size distribution. As a result, neither kind of observation can really be considered as real time. Therefore, in the context of aviation safety management, the utility of the approach described here can be seen in the following way. If we can use a combination of satellite observations to obtain plume height, on the one hand and the factor f on the other hand, a library of calculations based on the model we have presented can be rapidly used to estimate the flux of ash being injected at the source and input into the dispersion model. By this means one can hope to obtain a forecast of ash concentration distribution up to a day or so ahead of time and hence use this information to minimize disruption or cancellations of air traffic.

[36] **Acknowledgments.** We thank Lori Glaze, Larry Mastin, and an anonymous reviewer for their positive and constructive comments that helped to improve the paper. This work was carried out under the framework of the GMES project EVOSS, "European Volcano Observatory Space Services," funded in the 2nd Space Call of the 7th Framework Program of the European Commission, with grant agreement 242535. EVOSS started on 1 March 2010.

References

Burgisser, A., and J. E. Gardner (2005), Experimental constraints on degassing and permeability in volcanic conduit flow, *Bull. Volcanol.*, *67*, 42–56.

Bursik, M. (2001), Effect of wind on the rise height of volcanic plumes, *Geophys. Res. Lett.*, *28*, 3621–3624.

Bursik, M. I., and A. W. Woods (1996), The dynamics and thermodynamics of large ash flows, *Bull. Volcanol.*, *58*, 175–193.

Carazzo, G., E. Kaminski, and S. Tait (2006), The route to self-similarity in turbulent jets and plumes, *J. Fluid. Mech.*, *547*, 137–148.

Carazzo, G., E. Kaminski, and S. Tait (2008a), On the rise of turbulent plumes: Quantitative effects of variable entrainment for submarine hydrothermal vents, terrestrial and extra terrestrial explosive volcanism, *J. Geophys. Res.*, *113*, B09201, doi:10.1029/2007JB005458.

Carazzo, G., E. Kaminski, and S. Tait (2008b), On the dynamics of volcanic columns: A comparison of field data with a new model of negatively buoyant jets, *J. Volcanol. Geotherm. Res.*, *178*, 94–103.

Chouet, B., N. Hamisevicz, and T. R. McGetchin (1974), Photoballistics of volcanic jet activity at Stromboli, Italy, *J. Geophys. Res.*, *79*, 4961–4976.

Cioni, R., A. Longo, G. Macedonio, R. Santacroce, A. Sbrana, R. Sulpizio, and D. Andronico (2003), Assessing pyroclastic fall hazard through field data and numerical simulations: Example from Vesuvius, *J. Geophys. Res.*, *108*(B2), 2063, doi:10.1029/2001JB000642.

Clarisse, L., F. Prata, J.-L. Lacour, D. Hurtmans, C. Clerbaux, and P.-F. Coheur (2010), A correlation method for volcanic ash detection using hyperspectral infrared measurements, *Geophys. Res. Lett.*, *37*, L19806, doi:10.1029/2010GL044828.

Corradini, S., L. Merucci, A. J. Prata, and A. Piscini (2010), Volcanic ash and SO_2 in the 2008 Kasatochi eruption: Retrievals comparison from different IR satellite sensors, *J. Geophys. Res.*, *115*, D00L21, doi:10.1029/2009JD013634.

Esposti Ongaro, T., A. Neri, G. Menconi, M. de'Michieli Vitturi, P. Marianelli, C. Cavazzoni, G. Erbacci, and P. J. Baxter (2008), Transient 3D numerical simulations of column collapse and pyroclastic density current scenarios at Vesuvius, *J. Volcanol. Geotherm. Res.*, *178*, 378–396, doi:10.1016/j.jvolgeores.2008.06.036.

Glaze, L. S., and S. M. Baloga (1996), Sensitivity of buoyant plume heights to ambient atmospheric conditions: Implications for volcanic eruption columns, *J. Geophys. Res.*, *101*, 1529–1540.

Glaze, L. S., S. M. Baloga, and L. Wilson (1997), Transport of atmospheric water vapor by volcanic eruption columns, *J. Geophys. Res.*, *102*, 6099–6108.

Gouhier, M., and F. Donnadieu (2008), Mass estimations of ejecta from Strombolian explosions by inversion of Doppler radar measurements, *J. Geophys. Res.*, *113*, B10202, doi:10.1029/2007JB005383.

Harris, A. J. L., J. Dehn, and S. Calvari (2007), Lava effusion rate definition and measurement: A review, *Bull. Volcanol.*, *70*, 1–22, doi:10.1007/s00445-007-0120-y.

Hirn, B., C. Di Bartola, and F. Ferrucci (2009), Combined use of SEVIRI and MODIS for detecting, measuring, and monitoring active lava flows at erupting volcanoes, *IEEE Trans. Geosci. Remote Sens.*, *47*, 2923–2930.

Kaminski, E., and C. Jaupart (1997), Expansion and quenching of vesicular magma fragments in Plinian eruptions, *J. Geophys. Res.*, *102*, 12,187–12,203.

Kaminski, E., and C. Jaupart (1998), The size distribution of pyroclasts and the fragmentation sequence in explosive volcanic eruptions, *J. Geophys. Res.*, *103*, 29,759–29,779.

Kaminski, E., and C. Jaupart (2001), Marginal stability of atmospheric eruption columns and pyroclastic flow generation, *J. Geophys. Res.*, *106*, 21,785–21,798.

Kaminski, E., S. Tait, and G. Carazzo (2005), Turbulent entrainment in jets with arbitrary buoyancy, *J. Fluid. Mech.*, *526*, 361–376.

Klug, C., and K. V. Cashman (1996), Permeability development in vesiculating magmas: Implications for fragmentation, *Bull. Volcanol.*, *58*, 87–100.

Lane, S. J., and J. S. Gilbert (1992), Electric potential gradient changes during explosive activity at Sakurajima volcano, Japan, *Bull. Volcanol.*, *54*, 590–594.

Mastin, L. G., et al. (2009), A multidisciplinary effort to assign realistic source parameters to models of volcanic ash-cloud transport and dispersion during eruptions, *J. Volcanol. Geotherm. Res.*, *186*, 10–21, doi:10.1016/j.jvolgeores.2009.01.008.

Mastin, L. G., H. Schwaiger, and R. P. Denlinger (2010), Why do models predict such large ash clouds? An investigation using data from the Eyjafjallajökull eruption, Iceland, Abstract V54C-03 presented at 2010 Fall Meeting, AGU, San Francisco, Calif., 13–17 Dec.

Morton, B. R., G. Taylor, and J. S. Turner (1956), Turbulent gravitational convection from maintained and instantaneous sources, *Proc. R. Soc. London, Ser. A*, *234*, 1–23.

Neri, A., T. Esposti Ongaro, G. Menconi, M. De Michieli Vitturi, C. Cavazzoni, G. Erbacci, and P. J. Baxter (2007), 4D simulation of explosive dynamics at Vesuvius, *Geophys. Res. Lett.*, *34*, L04309, doi:10.1029/2006GL028597.

Petersen, G. N. (2010), A short meteorological overview of the Eyjafjallajökull eruption 14 April–23 May 2010, *Weather*, *65*, 203–207.

Piscini, A., S. Corradini, L. Merucci, and S. Scollo (2010), The 2010 Eyjafjallajökull eruption evolution by using IR satellite sensor measurements: Retrieval comparison and insights into explosive volcanic processes, Abstract V41E-2318 presented at 2010 Fall Meeting, AGU, San Francisco, Calif., 13–17 Dec.

Rose, W. I., and A. J. Durant (2009), Fine ash content of explosive eruptions, *J. Volcanol. Geotherm. Res.*, *186*, 32–39.

Rose, W. I., R. L. Chuan, R. D. Cadle, and D. C. Woods (1980), Small particles in volcanic eruption clouds, *Am. J. Sci.*, *280*, 671–696.

Sparks, R. S. J. (1986), The dimensions and dynamics of volcanic eruption columns, *Bull. Volcanol.*, *48*, 3–15.

Suzuki, Y. J., and T. Koyaguchi (2009), A three-dimensional numerical simulation of spreading umbrella clouds, *J. Geophys. Res.*, *114*, B03209, doi:10.1029/2007JB005369.

Textor, C., H. F. Graf, M. Herzog, and J. M. Oberhuber (2003), Injection of gases into the stratosphere by explosive volcanic eruptions, *J. Geophys. Res.*, *108*(D19), 4606, doi:10.1029/2002JD002987.

Thomas, H. E., and A. J. Prata (2011), Sulphur dioxide as a volcanic ash proxy during the April–May 2010 eruption of Eyjafjallajökull volcano, Iceland, *Atmos. Chem. Phys. Discuss.*, *11*, 7757–7780, doi:10.5194/acpd-11-7757-2011.

Thomas, N., C. Jaupart, and S. Vergniolle (1994), On the vesicularity of pumice, *J. Geophys. Res.*, *99*, 15,633–15,644.

Tupper, A., and R. Wunderman (2009), Reducing discrepancies in ground and satellite-observed eruption heights, *J. Volcanol. Geotherm. Res.*, *186*, 22–31.

Tupper, A., S. Carn, J. Davey, Y. Kamada, R. Potts, F. Prata, and M. Tokuno (2004), An evaluation of volcanic cloud detection techniques during recent significant eruptions in the western "Ring of Fire," *Remote Sens. Environ.*, *91*, 27–46, doi:10.1016/j.rse.2004.02.004.

Veitch, G., and A. W. Woods (2002), Particle recycling in volcanic plumes, *Bull. Volcanol.*, *64*, 31–39.

Wilson, L., R. S. J. Sparks, T. C. Huang, and N. D. Watkins (1978), The control of volcanic column heights by eruption energetics and dynamics, *J. Geophys. Res.*, *83*, 1829–1836.

Witham, C. S., M. C. Hort, R. Potts, R. Servranckx, P. Husson, and F. Bonnardot (2007), Comparison of VAAC atmospheric dispersion models using the 1 November 2004 Grimsvötn eruption, *Meteorol. Appl.*, *14*, 27–38.

Wright, R., S. Blake, A. J. L. Harris, and D. A. Rothery (2001), A simple explanation for the space-based calculation of lava eruption rates, *Earth Planet. Sci. Lett.*, *192*, 223–233.

Woods, A. W. (1988), The fluid dynamics and thermodynamics of eruption columns, *Bull. Volcanol.*, *50*, 169–193.

Woods, A. W. (1993), A model of the plumes above basaltic fissure eruptions, *Geophys. Res. Lett.*, *20*, 1115–1118.

Woods, A. W. (1995), The dynamics of explosive volcanic eruptions, *Rev. Geophys.*, *33*, 495–530.

F. Ferrucci, E. Kaminski, and S. Tait, Institut de Physique du Globe, 1 rue Jussieu, F-75238 Paris CEDEX 5, France. (fferrucci@ipgp.fr; kaminski@ipgp.fr; tait@ipgp.fr)

B. Hirn, IES Consulting, 34 via di San Valentino, I-00197 Rome, Italy. (b.hirn@iesconsulting.net)

P. Husson and M. Martet, VAAC Toulouse, Météo France, 42 avenue Gaspard Coriolis, F-31057 Toulouse CEDEX 1, France. (philippe.husson@meteo.fr; maud.martet@meteo.fr)